Title No. 114-S18

Shear Behavior and Crack Control Characteristics of Hybrid Steel Fiber-Reinforced Concrete Panels

by Stamatina G. Chasioti and Frank J. Vecchio

This paper investigates the beneficial influence of fiber hybridization on the shear strength of prismatic elements in terms of strength, deformation capacity, and cracking properties. Fourteen tests were performed using the Panel Element Tester Facility at the University of Toronto. Hooked-end steel macrofibers and straight short microfibers were combined in a normal-strength concrete matrix. The parameters examined were: the total fiber volumetric ratio, the performance of hybrid steel fiber-reinforced concrete (HySFRC) versus its single fiber counterparts with the same total amount of fibers, the effect of cyclic loading, the influence of pre-cracking in longitudinal tension on shear response, and the effect of biaxial tensile stresses combined with shear. Test results showed that shear strength and effective stiffness were enhanced through fiber hybridization. For example, in panels having a total fiber volumetric ratio of 1.5%, the HySFRC panel exhibited a 10% enhancement in shear strength compared to its counterpart with macrofibers only. Synergy in shear increased with increasing fiber ratio. Crack widths and spacing were not affected by load reversals.

Keywords: cyclic; initial damage; panels; shear; steel fibers; synergy.

INTRODUCTION

Fiber-reinforced concrete has been under investigation for more than 50 years, with research outcomes having served as the basis for the development of concretes used in a wide range of applications. For structural purposes, it has been used as partial or full replacement of conventional reinforcement in force-resisting members. It is also used in industrial floors and façades, for non-structural purposes, and in tunnel linings and concrete pavements for special category projects.[1,2] With the development of the concrete technology, the resulting materials have been made more durable, leading to increased energy absorption; these composites are commonly referred to as high-performance fiber-reinforced cementitious composites (HPFRCC).

The complete behavior of the concrete composite, as well as the range of the fiber effectiveness, depends on three parameters. These are: the cementitious matrix (its constituents and their relative ratio), the fiber (its elastic modulus and geometric properties), and the bond that defines the state of stress between the matrix and the fiber.[3] Over the years, studies have demonstrated how the fiber characteristics, in terms of material and geometry, influence the concrete properties, and empirical rules have been developed accordingly.[1-5] Hybrid steel fiber-reinforced concrete (HySFRC) attempts to take advantage of the different fiber contributions by combining them. In well-designed hybrid composites, the response is not simply the addition of separate fiber contributions, but rather the constitutive properties of the material

exceeding those of the corresponding monofiber concretes. Hybridization is essentially an optimization process and the positive interaction between the fibers is often termed as "synergy."

Many combinations have been tested so far, and they are generally summarized under three main categories[1-5]:

- *Hybrids based on the fiber constitutive response:* Fibers with high moduli of elasticity are considered effective in bridging microcracks, while ones with low moduli are mobilized at larger crack openings.

- *Hybrids based on fiber dimensions and the anchorage mechanism*: Microfibers (short fibers) have been proven to arrest the coalescence of cracks at an early stage conditionally leading to strength increase, while the macrofibers (longer fibers) help increase the post-cracking toughness. Their effectiveness depends on the anchorage mechanism.[6-8]

- *Hybrids based on the fiber function*: this category involves fibers both for the improvement of the mechanical and early age properties.

Taking into account the complexity and the large number of parameters affecting the response of HPFRCC, in 2003, Naaman and Reinhardt[9] proposed the classification of HPFRC composites based on their performance in direct tension and bending. Furthermore, in 2006,[10] they identified the need that specific performance criteria should be met within the aforementioned categories for structural applications. Strain-hardening materials, for example, should meet a value for the strain at the peak stress in tension of at least 0.005, so they sufficiently contribute to the nominal bending resistance. Later, in 2009, Blunt and Ostertag[11] proposed that deflection-hardening materials should maintain the matrix tensile strength across a growing crack through the yield strain of the reinforcing bar (an average tensile strain capacity of 0.002), setting ductility as the first priority. It is worth noting that both criteria refer to the steel strain with respect to members in bending. Although setting performance requirements is necessary for the broader, more effective, and safer use of the materials, efforts are also needed with respect to the shear behavior of such composites.

The behavior of the composite under shear loading is particularly important for structural applications. Crack control and a ductile failure mode for structural members, including under shear-dominated conditions, are the main reasons that made fibers attractive to structural engineers in the first place. Many beams have been tested examining the influence of the fiber percentage, fiber aspect ratio, longitudinal reinforcement ratio, and concrete strength on the shear behavior.[12-14] It was found that inclusion of fibers resulted in increased shear resistance, ductility, and smaller crack widths. Some test results showed that it also altered the failure mode from brittle to ductile with yielding of the longitudinal reinforcement. In 2006, Parra-Montesinos[15] compiled a database of 147 beams, which formed the basis for acceptance of steel fibers as an alternative to minimum shear reinforcement for the first time in ACI 318-08.[16] Beams with 0.75% deformed steel fibers withstood at least $0.3\sqrt{f_c'}$ ($3.5\sqrt{f_c'}$ in psi) shear stress. To ensure adequate material performance, criteria on the post-cracking behavior based on flexural tests per ASTM C1609[17] were further imposed. The idea of linking the shear strength of fiber-reinforced concrete to the post-cracking toughness in tension indirectly by flexural tests, given the lack of a reliable direct tension specimen, had also been introduced in 2003 by the RILEM TC 162-TDF recommendations.[18] Earlier, in 1994, Li et al.[19] identified the need for a link to be established between the shear behavior on a structural component level and the concrete composite properties. Although benefits in shear due to fiber inclusion have thus been established, HySFRC may be an interesting extension of the concept.[20,21]

Work presented herein is part of a larger study whose purpose is to examine the so-called synergy between fibers, both at the material and structural levels, in terms of strength, displacement capacity and failure mode. Hence, the main focus of this paper is the shear behavior of hybrid steel fiber reinforced concrete panels with conventional reinforcement. Potential benefits due to synergy from combining two different types of steel fibers with respect to the shear strength are examined. Hooked-end steel macrofibers, straight short microfibers, and normal-strength concrete matrix form the basis of the constitutive cementitious material.

RESEARCH SIGNIFICANCE

Optimization of the fiber combination so that fracture is restrained on multiple levels leads to concrete with enhanced mechanical characteristics. Although benefits in shear due to fiber inclusion have already been established, HySFRC may be an interesting advancement potentially leading to increased shear strength and crack control characteristics for the same fiber volumetric ratio. Cost and conventional steel reinforcement congestion could be further reduced due to synergistic effects attained through fiber hybridization. Moreover, hybridization potentially offers flexibility in the constitutive characteristics of the basic mechanical properties of concrete, particularly useful for targeted concrete designs satisfying specific needs.
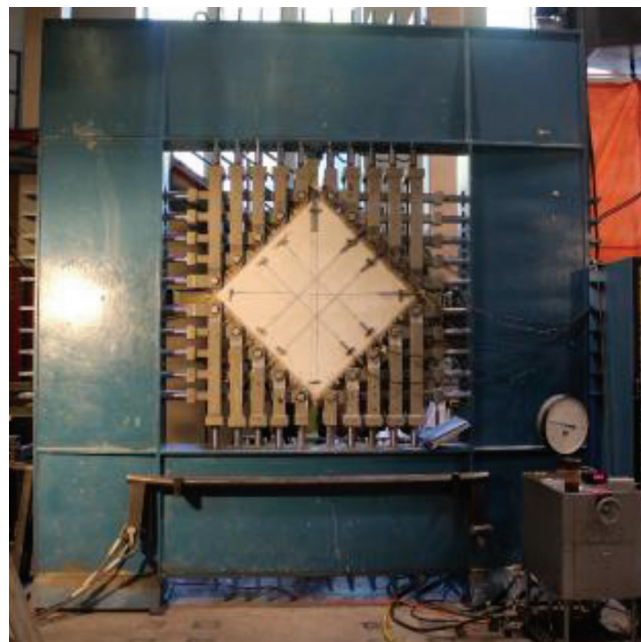

Fig. 1—Panel element tester facility at University of Toronto.

EXPERIMENTAL INVESTIGATION

This study aims to examine the potential benefits due to fiber synergy under shear loading in HySFRC specimens reinforced with conventional steel bars. The goal is evaluated in terms of strength, ductility, deformation, hysteretic behavior and crack control characteristics. Hybrid specimens containing two types of steel fibers in a 1:1 ratio were compared against their single-fiber counterparts with the same total amount of fibers. Fourteen panel specimens were tested in total; 12 under pure shear in-plane loading conditions, and two under shear and biaxial tension. The tests were performed using the Panel Element Tester facility at the University of Toronto (Fig. 1). The test matrix adopted is shown in Table 1. Five variables were examined: total fiber volumetric fraction V_f; the performance of the HySFRC specimens versus monofiber counterparts with the same total amount of fibers; the performance of panels tested under monotonic pure shear versus reversed cyclic shear loading; panels that were cracked in longitudinal tension prior to shear loading versus panels initially uncracked prior to loading in shear; and the influence of proportionally increasing biaxial tension and shear on the panel response. The specimen notation adopted is as follows: first index—H for hybrid fibers in a ratio 1:1, SL for single type of fiber-long (macrofiber), and SS for single type of fiber-short (microfiber); second index—the total V_f, equal to 0.75%, 1.0%, 1.5%, and 2.0%; third index—PS for pure shear (no co-acting normal stresses) and ST for shear and proportionally increasing biaxial tension in a ratio 1:0.5; and fourth index—M for monotonic-positive shear loading and C for reversed cyclic shear loading. Although many other types and lengths of fiber can be combined, this paper focuses on just one combination to illustrate potential benefits.

Table 1—Test matrix

Specimen	Fiber configuration	Total V_f, %	Loading	Type of loading
H1.5PSM	Hybrid	1.5	Pure shear	Monotonic
H1.5PSC	Hybrid	1.5	Pure shear	Reversed cyclic
SL1.5PSC	Macrofiber only	1.5	Pure shear	Reversed cyclic
SS1.5PSC	Microfiber only	1.5	Pure shear	Reversed cyclic
H1.0PSM	Hybrid	1.0	Pure shear	Monotonic
H1.0PSC	Hybrid	1.0	Pure shear	Reversed cyclic
SL1.0PSC	Macrofiber only	1.0	Pure shear	Reversed cyclic
SS1.0PSC	Microfiber only	1.0	Pure shear	Reversed cyclic
H1.5PSM-predamaged	Hybrid	1.5	Pure shear	Monotonic
H1.5PSC-predamaged	Hybrid	1.5	Pure shear	Reversed cyclic
H1.0STM	Hybrid	1.0	Shear and biaxial tension	Monotonic
H1.0STC	Hybrid	1.0	Shear and biaxial tension	Reversed cyclic
H0.75PSM	Hybrid	0.75	Pure shear	Monotonic
H2.0PSM	Hybrid	2.0	Pure shear	Monotonic

Table 2—Mixture design

Material	Hy0.75	Hy1.0	SL1.0	SS1.0	Hy1.5	SL1.5	SS1.5	Hy2.0
Cement, kg/m³ (lb/ft³)	432 (26.96)	432 (26.96)	432 (26.96)	432 (26.96)	432 (26.96)	432 (26.96)	432 (26.96)	432 (26.96)
Water, kg/m³ (lb/ft³)	194 (12.11)	194 (12.11)	194 (12.11)	194 (12.11)	194 (12.11)	194 (12.11)	194 (12.11)	194 (12.11)
Sand, kg/m³ (lb/ft³)	972 (60.68)	972 (60.68)	972 (60.68)	972 (60.68)	972 (60.68)	972 (60.68)	972 (60.68)	972 (60.68)
Coarse aggregate, kg/m³ (lb/ft³)	798 (49.82)	792 (49.44)	792 (49.44)	792 (49.44)	778 (48.57)	778 (48.57)	778 (48.57)	764 (47.69)
Microfibers/macrofibers, kg/m³ (lb/ft³)	29.5/29.5 (1.84/1.84)	39/39 (2.4/2.4)	78 (4.87)	78 (4.87)	58.5/58.5 (3.65/3.65)	117 (7.30)	117 (7.30)	78/78 (4.87/4.87)
High-range water-reducing admixture, mL (oz)	4.5 (4.5)	5 (5)	4 (4)	3.75 (3.75)	8.2 (8.2)	7.9 (7.9)	7.9 (7.9)	8.2 (8.2)

Constitutive materials

The mixture design of all eight composites is shown in Table 2. GUL cement was used as the binder. The water-cement ratio (w/c) was kept constant at 0.45. Washed coarse aggregate with a maximum size of 9.5 mm (3/8 in.) was graded according to CSA A23.1-09/A23.2-09.[22] The concrete matrix was the same for all composites for comparison purposes.

Two types of high-strength steel fibers, different in terms of geometry (that is, length, aspect ratio, and anchorage mechanism), were used. Table 3 summarizes their pertinent fiber properties and geometric characteristics. The RC-80/30-BP hooked-end fibers and the straight OL13/.20 served as the macrofibers and the microfibers, respectively, in a ratio 1:1 for the hybrid mixtures. Conventional steel reinforcing bars were included in the panel specimens. The reinforcing bars were made of cold-formed steel, with a yield stress of 520 MPa (75.4 ksi), essentially following an elasto-plastic

Table 3—Fiber properties and geometry

Fiber	l_f, mm (in.)	d_f, mm (in.)	AR_f	f_{uf}, MPa (ksi)	E_f, MPa (ksi)
RC80/30BP	30 (1-3/16)	0.38 (0.015)	79	3070 (445.2)	200,000 (29,000)
OL13/.20	13 (33/64)	0.21 (0.008)	62	2750 (398.8)	200,000 (29,000)

stress-strain law until fracture. The steel properties are given in Table 4.

Specimens

Concrete was mixed using a high-energy mixer in the materials lab at the University of Toronto. All specimens were consolidated under external vibration attached to the steel molds. Once cast, they were moist-cured for 7 days, covered with burlap and plastic sheets. Twenty-one days

Table 4—Conventional steel reinforcement properties

Reinforcing bar type	d_b, mm (in.)	A_s, mm² (in.²)	E_s, GPa (ksi)	f_y, MPa (ksi)	ε_y, × 10^{-3}	f_u, MPa (ksi)	ε_u, × 10^{-3}
D8	8.10 (3/8)	51.5 (0.08)	200 (29,007)	520 (75.4)	2.6	520 (75.4)	35

Table 5—Summary test results

ID	$f_{ck,100}$, MPa (ksi)*	v_{cr}, MPa (ksi)	γ_{cr}, x10^{-3}	v^+_u, MPa (ksi)	γ^+_u, x10^{-3}	v^-_u, MPa (ksi)	γ^-_u, x10^{-3}	w_{max}, mm (in.)	s_m, mm (in.)	Failure mode
H1.5PSM	41.56 (6.02)	3.50 (0.51)	0.35	6.15 (0.89)	6.30	—	—	0.4 (0.015)	64 (2.52)	x-reinforcement rupture
H1.5PSC	55.48 (8.05)	3.50 (0.51)	0.33	5.75 (0.83)	2.71	−5.70 (−0.83)	−2.83	0.3 (0.012)	63 (2.48)	Premature edge failure
SL1.5PSC	61.13 (8.87)	2.00 (0.29)	0.20	5.29 (0.77)	4.53	−5.59 (−0.81)	−3.96	0.7 (0.028)	67 (2.64)	Shear slip
SS1.5PSC	50.46 (7.32)	3.25 (0.47)	0.22	4.81 (0.70)	1.72	−4.56 (−0.66)	−3.53	0.7 (0.028)	103 (4.06)	Shear slip
H1.0PSM	51.34 (7.45)	3.25 (0.47)	0.33	5.02 (0.73)	3.99	—	—	0.25 (0.01)	68 (2.68)	Shear slip
H1.0PSC		3.0 (0.44)	0.27	4.82 (0.70)	3.69	−4.83 (−0.70)	−5.21	0.5 (0.02)	71 (2.80)	Shear slip
SL1.0PSC	57.53 (8.34)	2.75 (0.40)	0.21	4.58 (0.66)	3.59	−4.57 (−0.66)	−4.97	0.25 (0.01)	74 (2.91)	Shear slip
SS1.0PSC	54.12 (7.85)	3.0 (0.44)	0.26	4.34 (0.63)	3.96	−4.34 (−0.63)	−3.69	0.3 (0.012)	71 (2.80)	Shear slip
H1.5PSM-predamaged	71.69 (10.40)	4.0 (0.58)	0.41	6.59 (0.96)	5.0	—	—	0.2 (0.008)	68 (2.68)	Shear slip
H1.5PSC-predamaged		3.5 (0.51)	0.34	5.76 (0.84)	4.08	−5.76 (−0.84)	−3.98	0.2 (0.008)	71 (2.80)	Shear slip
H1.0STM	63.49 (9.21)	2.0 (0.29)	0.18	3.19 (0.46)	1.46	—	—	0.2 (0.008)	137 (5.39)	Shear slip
H1.0STC		2.0 (0.29)	0.06	3.19 (0.46)	1.51	−2.98 (−0.43)	−0.75	0.15 (0.006)	71 (2.80)	Shear slip
H0.75PSM	60.97 (8.84)	3.50 (0.51)	0.27	5.27 (0.76)	4.85	—	—	0.4 (0.015)	71 (2.80)	Shear slip
H2.0PSM	58.16 (8.44)	3.25 (0.47)	0.32	6.63 (0.96)	8.65	—	—	0.4 (0.015)	56 (2.20)	Shear slip

*Obtained by 100 x 200 mm (4 x 8 in.) cylinder tests.

of dry curing in ambient lab conditions followed, prior to testing.

Cylinder tests were performed to evaluate the compressive stress of the concrete in accordance with ASTM C469/C469M.[23] The cylinders' dimensions were 100 mm (4 in.) in diameter and 200 mm (8 in.) in height. Values of the $f_{ck,100}$ are reported in Table 5.

Fourteen 890 x 890 x 70 mm (35 x 35 x 2.75 in.) panels were tested in total. Forty D8 deformed steel bars, in two layers, formed the longitudinal steel reinforcement, giving a ratio of 3.31% in the x-direction (ρ_x = 3.31%). Because the main purpose of the tests was the investigation of the shear behavior of concrete, no conventional transverse reinforcement was included; the hybrid steel fibers alone provided resistance in the y-direction (ρ_y = 0%). The high ρ_x steel ratio was selected so that yielding of the longitudinal steel would not impact the ultimate shear strength attainable. Yielding of the longitudinal steel would have limited the ability of the reinforcement to carry stress across a crack and hence cap

the principal tensile stress of concrete before it reached the peak. Forty 7.93 mm (5/16 in.) diameter high-strength steel threaded rods provide sufficient anchorage to the shear keys in the y-direction. The panel specimen geometry and layout is shown in Fig. 2.

Test setup and loading procedure

The tests were performed using the Panel Element Tester Facility (Fig. 1). Thirty-seven jacks and three rigid links comprised the hydraulic system that enables the user to apply any combination of shear and/or normal in-plane stresses. To prevent any out-of-plane movement due to the panel slenderness, an out-of-plane frame provided lateral support. Twenty shear keys around the specimen perimeter transferred the forces generated by the jacks. Each shear key was connected to two jacks, one in the vertical direction and one in the horizontal direction. A positive (+) pure shear loading condition was created when the vertical jacks advanced and the horizontal ones retracted with equal and
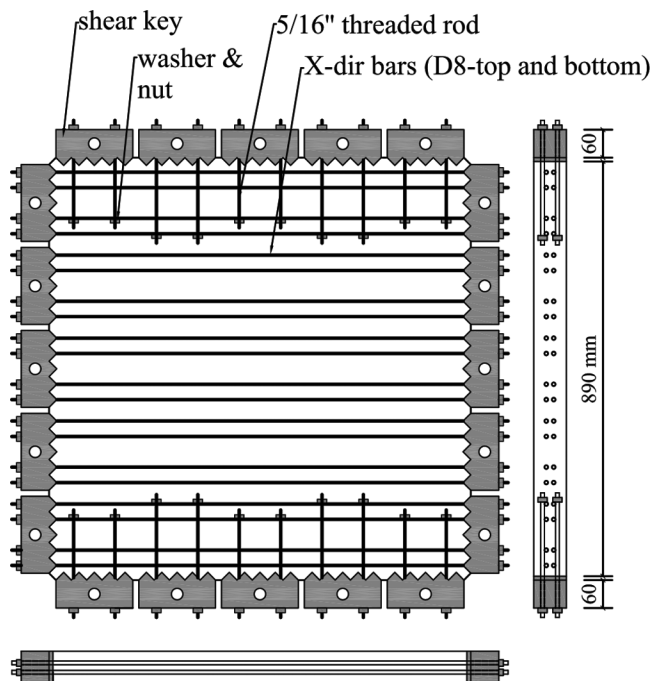
Fig. 2—Geometry and reinforcement layout of panel specimens. (Note: 1 mm = 0.039 in.)

opposite forces. In reversed cyclic loading, reversed directions constituted the negative shear condition.

The load was applied quasi-statically under load-control conditions. Two types of loading were considered: monotonic positive shear, and reversed cyclic shear. For the panels tested monotonically, the shear stress was incremented by steps of 0.25 MPa (0.036 ksi). For the reversed cyclic shear case, two cycles were performed at the same load level before incrementing by 0.25 MPa (0.036 ksi) to the next pair of cycles. Twelve panels were tested under pure in-plane shear conditions (no co-acting normal stresses), and two under combined shear and proportionally increasing biaxial tension in a ratio 1:0.5 (H1.0STM and H1.0STC). For the latter, the jack pressures in the vertical and the horizontal direction were appropriately adjusted. At each load stage, cracks were marked and their width was measured and updated.

Six linear variable displacement transducers (LVDTs) were mounted on both concrete surfaces, front and back. The LVDTs measured the displacements in the x-direction, y-direction, and the two diagonals, allowing the calculation of average normal and shear strains on the panel surfaces.

EXPERIMENTAL RESULTS

The test results are presented and discussed in this section. A summary of characteristic values obtained from the experiments are presented in Table 5. Values include the compressive strength of concrete obtained by cylinders, the shear stress and the corresponding shear strain at the onset of cracking; the maximum shear stress attained and the corresponding shear strain in the positive and negative directions; the maximum crack width measured at or before ultimate;

the average crack spacing at ultimate; and the failure mode. The onset of cracking for all of the panels occurred for the first time in the positive direction, and subsequently in the negative direction at about the same load level. All panels experienced limited crack rotation after the first crack formed at 45 degrees. SL1.5PSC was the only one that failed while being loaded in the negative direction. All except for two, as noted in Table 5, failed due to opening of the cracks followed by loss of the aggregate interlock shear transfer mechanism. Crack opening eventually occurred due to the inability of the fibers to effectively bridge and transmit load across them. Nevertheless, H1.5PSM was the only panel where rupture of the y-reinforcement occurred prior to shear slip failure. H1.5PSC failed somewhat prematurely in terms of ductility at ultimate, due to a connection edge failure, although it appeared to have reached its maximum capacity of 5.75 MPa (0.83 ksi) shear stress. Photographs of the specimens after failure are shown in Fig. 3 and 4. The results discussed herein are assessed in terms of strength, stiffness, deformation capacity, maximum crack width measured, and average crack spacing.

Influence of total fiber volumetric fraction

Figure 5(a) plots the shear stress versus strain for the panels tested under monotonic shear with V_f ranging from 0.75% to 2.0%. Up to the first crack, the behavior was almost identical among the panels. However, in the post-cracking responses, stiffness was seen to increase with increasing fiber volumetric ratio. Keeping in mind that higher amounts of fibers better restrain the cracks from opening, the higher fiber volume panels deformed less to reach equilibrium for the same load level. In addition, the panel that contained 2% hybrid fibers (H2.0PSM) attained the highest level of shear stress, at 6.63 MPa (0.96 ksi), and reached the highest deformation capacity at approximately 9×10^{-3} shear strain. Clearly, increasing the amount of steel fiber reinforcement resulted in progressive increases in the post-cracking stiffness, ultimate shear strength, and deformation capacity. H1.0PSM was somewhat affected by out-of-plane bending after it reached 4.5 MPa (0.65 ksi) and its stiffness dropped slightly just before it failed at 5.0 MPa (0.73 ksi) shear.

The shear stress versus the maximum crack width measured at each load stage, and the corresponding mean crack spacing, are presented in Fig. 5(b) and (c), respectively. As can be seen, cracking occurred at approximately 3.0 to 4.0 MPa (0.44 to 0.58 ksi) and the first cracks appear with a width of 0.05 mm (0.002 in.). As the shear stress increased, the crack widths appeared to be smaller for panels with increasing V_f, complementing the higher stiffness in shear. Although all panels had the same longitudinal steel layout, crack spacing appeared to be influenced by the V_f. Higher amounts of fibers promote smaller crack spacing. This was true both when cracking starts and after the crack stabilization. The point where the development of new cracks stopped (that is, stabilization) was delayed with increasing V_f.
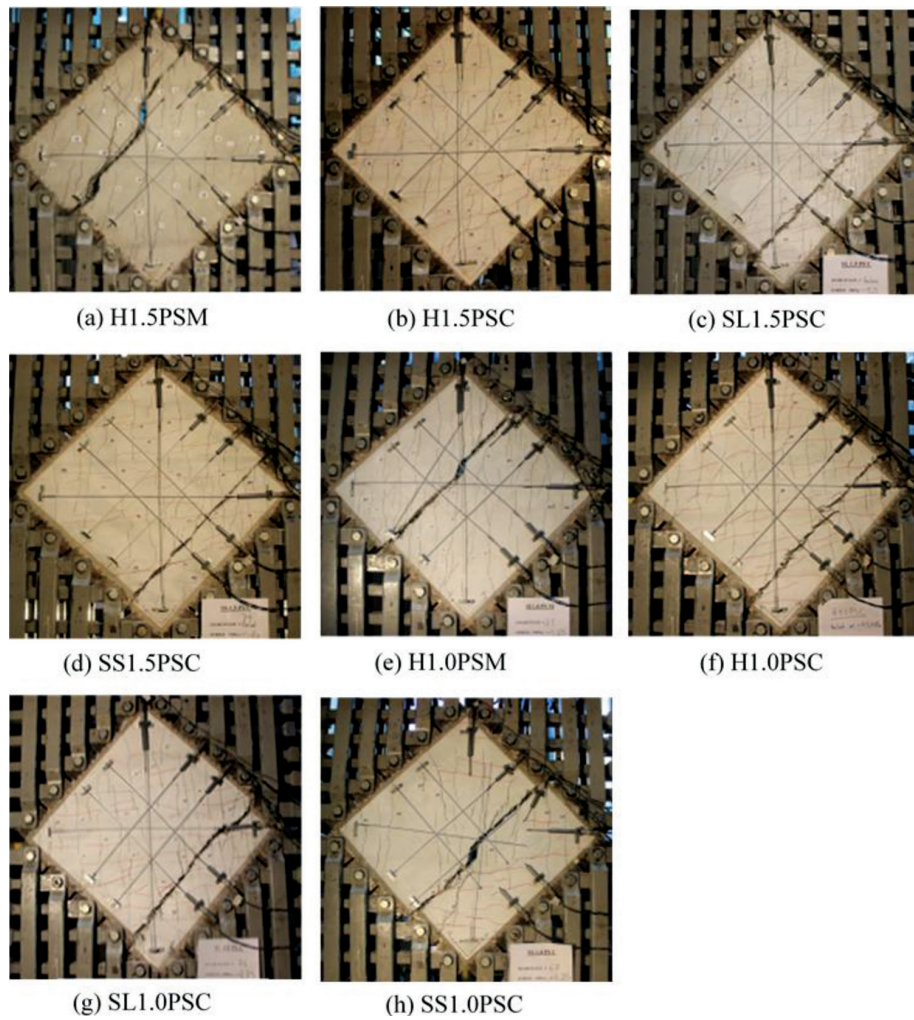
(a) H1.5PSM   (b) H1.5PSC   (c) SL1.5PSC

(d) SS1.5PSC   (e) H1.0PSM   (f) H1.0PSC

(g) SL1.0PSC   (h) SS1.0PSC

Fig. 3—Panel failure crack patterns (H1.5PSM to SS1.0PSC).

(a) H1.5PSM-predamaged   (b) H1.5PSC-predamaged   (c) H1.0STM
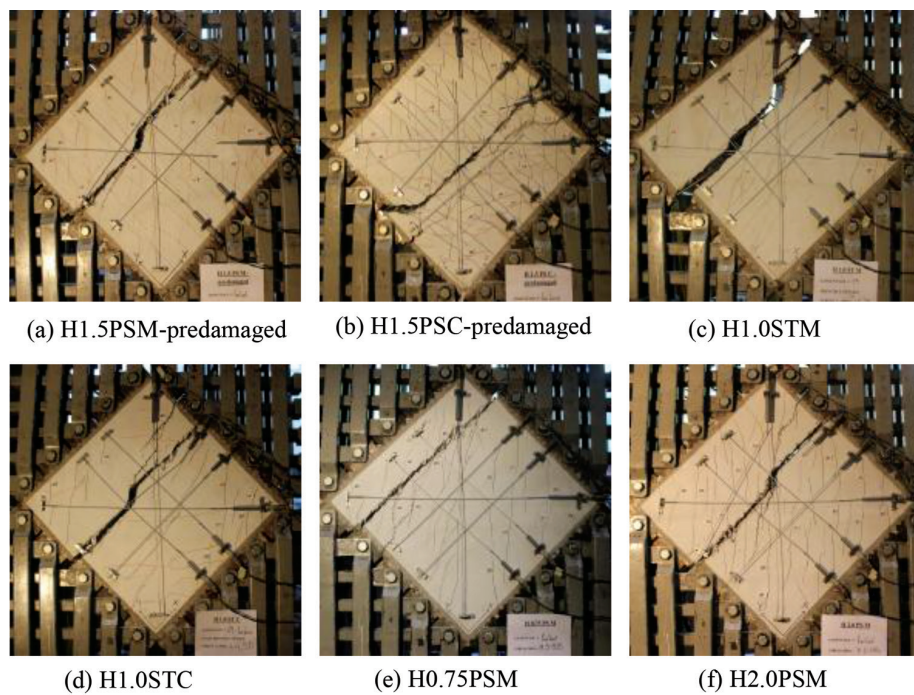
(d) H1.0STC   (e) H0.75PSM   (f) H2.0PSM

Fig. 4—Panel failure crack patterns (H1.5PSM-predamaged to H2.0PSM).
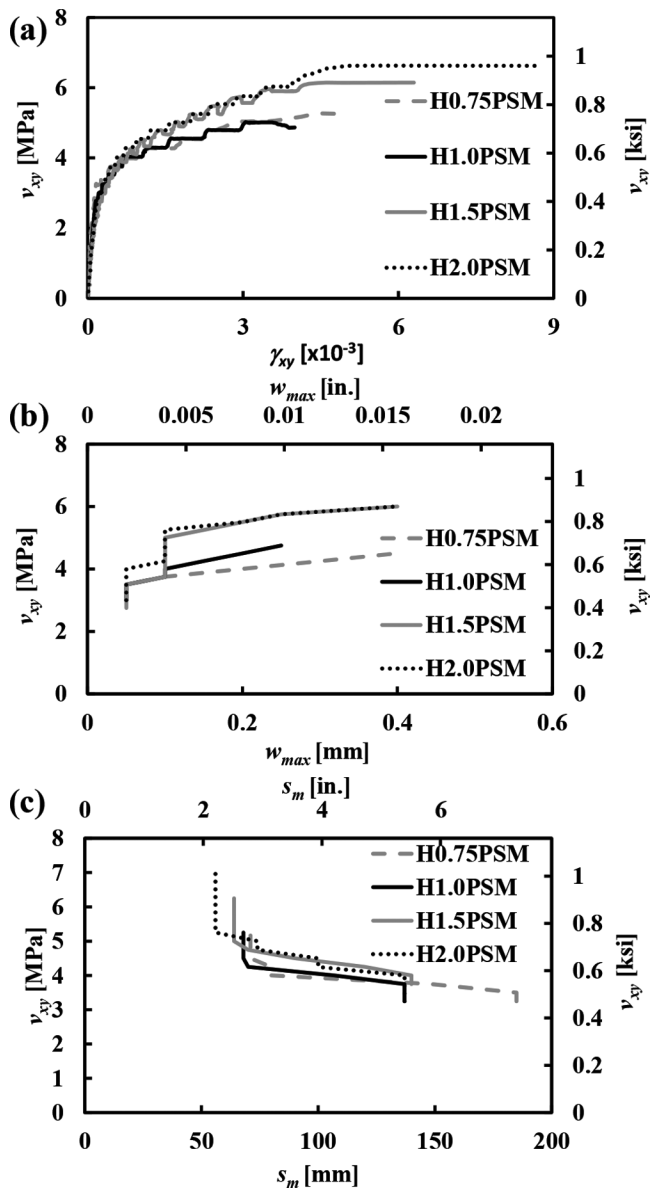
Fig. 5—Influence of V_f on panel shear response and cracking properties.

Fig. 6—Influence of hybridization for panels with $V_f = 1.5\%$.

HySFRC versus monofiber concrete

Figures 6(a) and (b) compare the shear response of hybrid-fiber concrete versus the long-fiber and short-fiber counterparts, respectively. Both figures show that the HySFRC achieved higher shear strength compared to the two mono-fiber concretes. Although H1.5PSC experienced a premature edge failure at 5.75 MPa (0.83 ksi), the capacity attained still represented a 10% enhancement compared to that of macro-fiber panel SL1.5PSC (5.25 MPa [0.76 ksi]) and a 20% enhancement over that of the microfiber panel SS1.5PSC (4.75 MPa [0.69 ksi]). Corresponding values for 1.0% hybrid fibers were approximately 7% and 11%, respectively. Thus, synergy in the shear strength increased with increasing fiber ratio.

H1.5PSM was stiffer in the post-cracking regime than SL1.5PSC, while SS1.5PSC appeared to be stiffer than both the other two. It reached the same load level at smaller deformation, and hence managed to limit its residual deformation
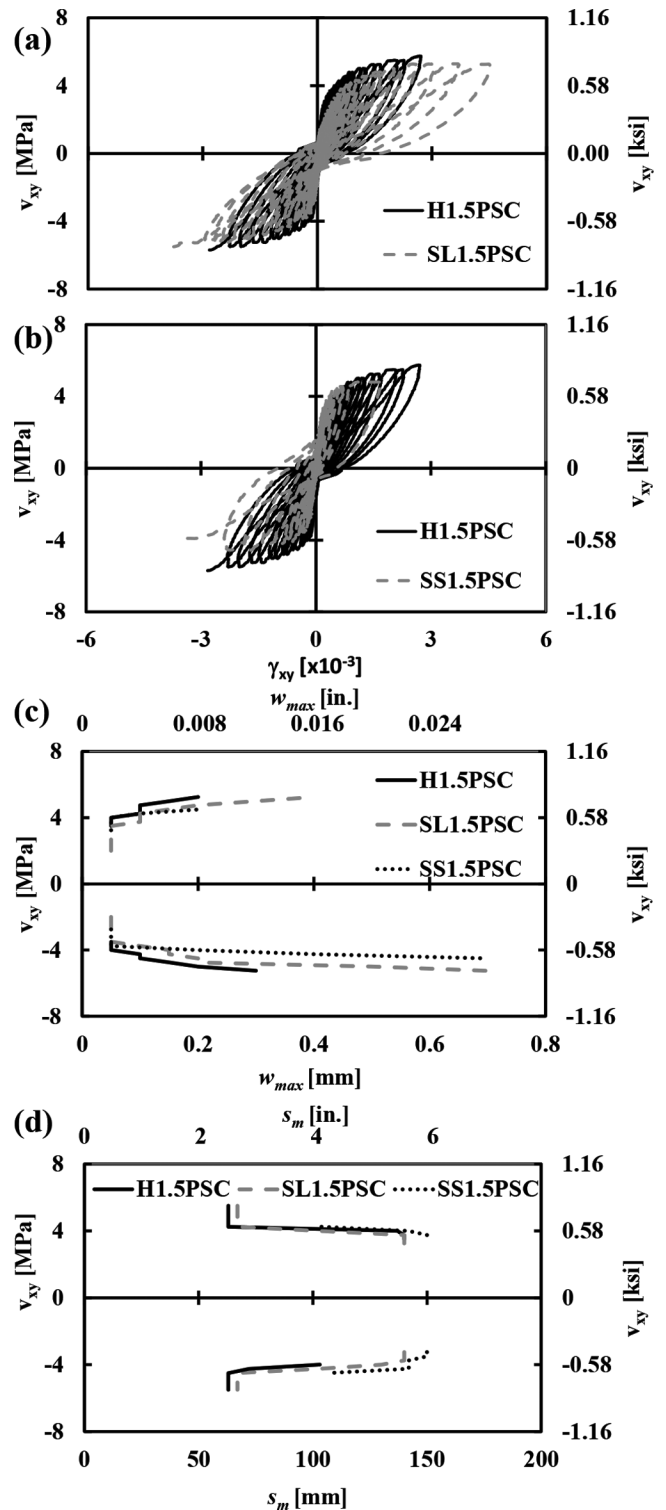
upon unloading. The shorter fibers were more effective at bridging smaller crack widths but experienced pullout soon thereafter because they could not support larger strains, thus resulting in limited ductility. Displacement capacity seems to be governed by the presence of long fibers, although no definitive conclusion can be drawn because H1.5PSC failed prematurely and H1.0PSC achieved slightly higher ultimate displacement despite containing only half of the SL1.0PSC long fibers (Fig. 7(a)). Hybrid concrete effectively managed
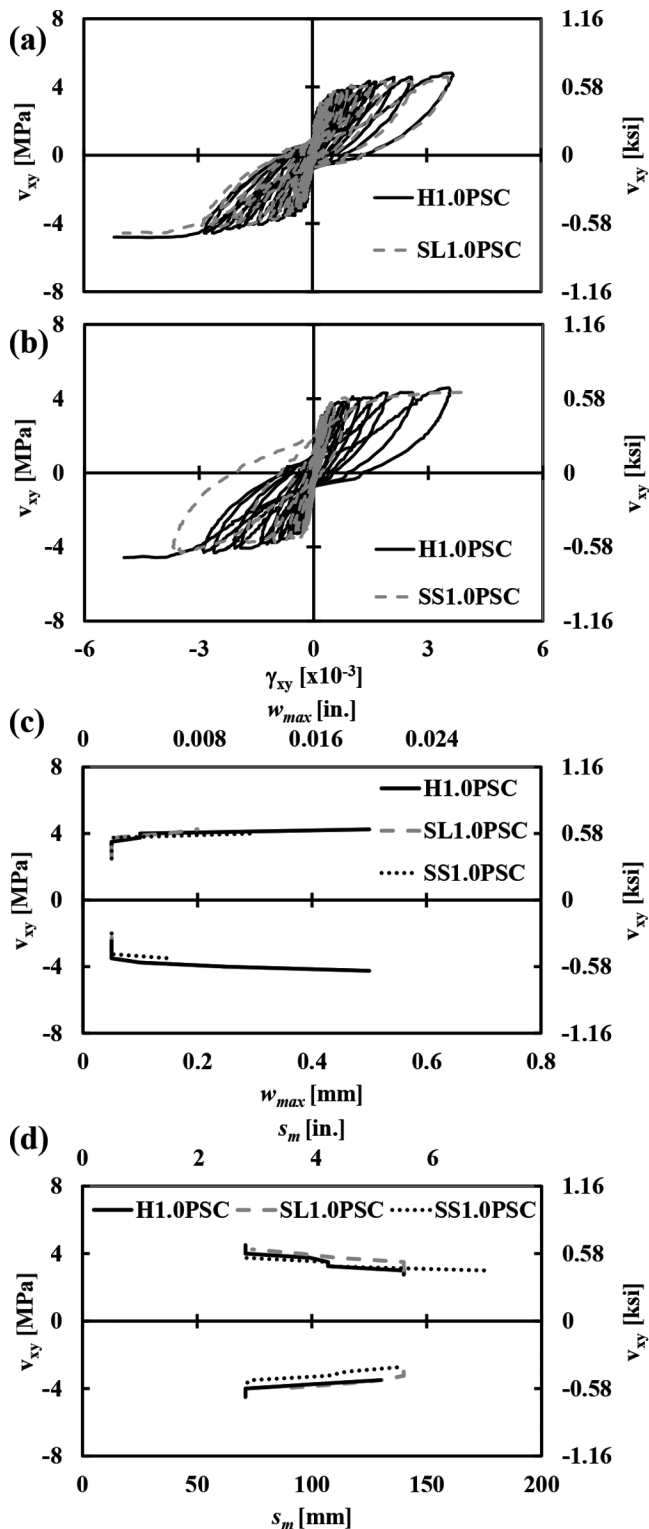
(a)

(b)

(c)

(d)

Fig. 7—Influence of hybridization for panels with $V_f = 1.0\%$.

to combine the benefits of the two different types of fibers and achieved at least the same maximum displacement while containing only half of the long fibers.

Thus, improved crack control, both at service load levels and at ultimate state, can be achieved through fiber hybridization (refer to Fig. 6(c) and (d) and 7(c) and (d)). Both crack widths and the crack spacing showed some reduction, with the effects being more pronounced with higher fiber

percentages (Fig. 6(c) and (d)). Stabilization occurred at approximately the same load level.

Monotonic versus reversed cyclic loading

Figure 8 shows the influence of load reversals on the shear response and cracking properties of hybrid concrete for various volumetric ratios (Fig. 8(a) to (f)) and load configurations (Fig. 9(a) to (f)). Panels tested under reversed cyclic shear showed a stable hysteretic response with energy dissipation. The reversed cyclic envelope followed the monotonic response for most of the loading protocol. Strength and deformation degradation due to cyclic damage accumulation appeared to take place during the last load steps before failure. H1.5PSC, which failed somewhat prematurely, experienced 6.5% degradation in strength capacity; the corresponding value for H1.0PSC was 4%.

Crack widths and spacings obtained from the monotonic tests were plotted both in the positive and negative directions for comparison purposes. It can be seen that crack widths and crack spacings were not much affected by the type of loading, as long as loading reached the same level. It should be noted, however, that crack widths were only measured while the cyclic curves were following the monotonic responses, for safety reasons. Once cyclic damage became apparent, the crack widths were observed to increase significantly and the panels were close to failure.

Influence of pre-cracking on shear behavior

The loading protocol for H1.5PSM-predamaged and H1.5PSC-predamaged consisted of two phases. In Phase I, the panels were loaded under uniaxial tension, in the longitudinal direction, up to a stress of 7.7 MPa (1.1 ksi). Multiple cracks appeared with an average spacing of 80 mm (3.15 in.) and average width of 0.05 mm (0.002 in.). Upon unloading, the cracks did not completely close and the residual tensile strain was 0.3×10^{-3}. Under Phase II testing, they were subjected to monotonic pure shear and reversed cyclic shear, respectively, to failure.

Figures 10(a) and (d) show the response of the panels in shear as compared to their undamaged counterparts. H1.5PSM-predamaged was seen to be somewhat stronger and stiffer than H1.5PSM. The cracks that formed in Phase I, oriented at a different angle than the cracks due to shear loading, resulted in a slight enhancement in shear strength, a phenomenon also reported by others.[24] Nevertheless, the deformation capacity was negatively affected. Under reversed cyclic shear loading, the strength enhancement effect was not observed. The behavior was almost the same up to 5.0 MPa (0.72 ksi), when the stiffness of H1.5PSC-predamaged began to drop. Although H1.5PSC failed prematurely, they both reached the same ultimate shear strength of 5.75 MPa (0.83 ksi).

The crack pattern at failure under shear was not affected by the presence of previous cracks, as shown in Fig. 4. Nevertheless, during the course of the experiment, the crack spacings were constantly somewhat larger, meaning less axial tensile strain demand on the reinforcement. The crack widths were also smaller. Overall, the tests results suggest
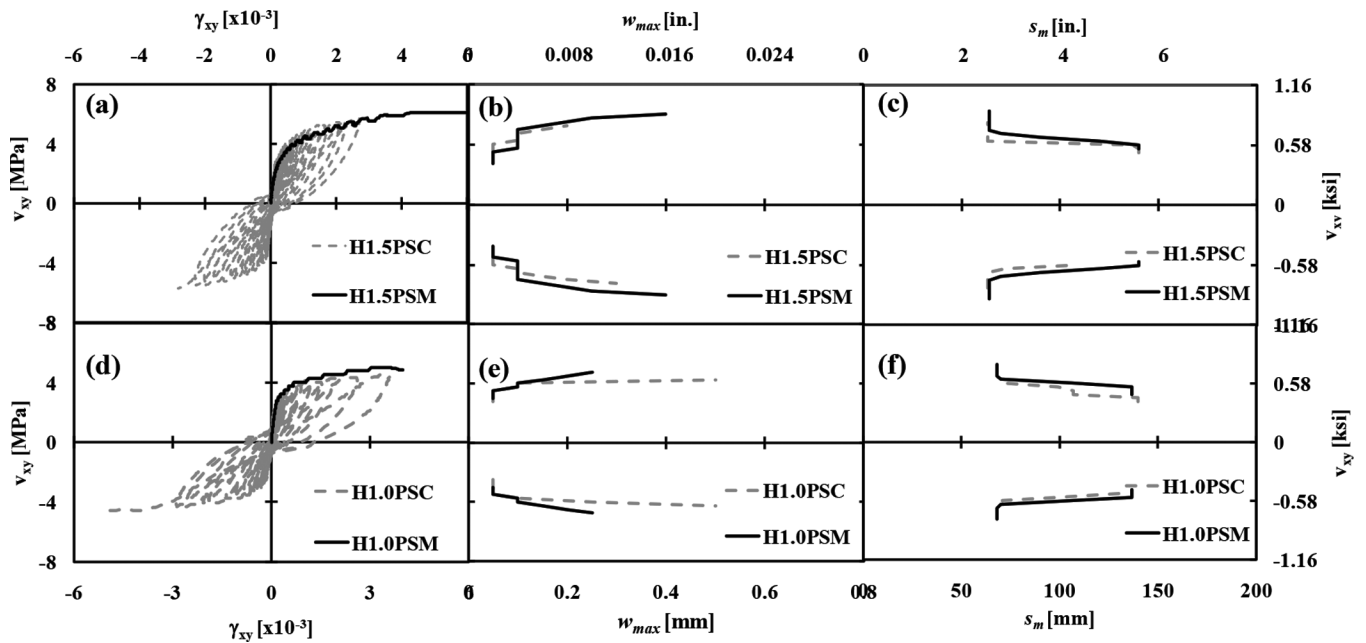
216

Fig. 8—Influence of cyclic loading on panel shear response and cracking properties for various volumetric ratios.
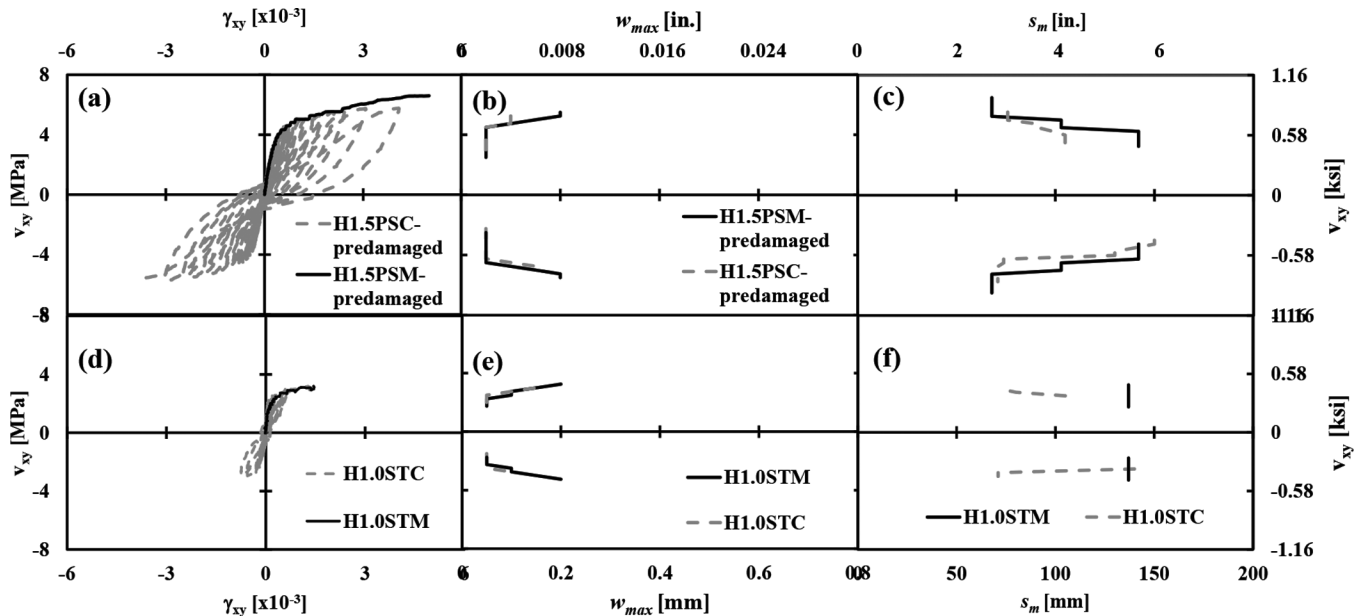

Fig. 9—Influence of cyclic loading on panel shear response and cracking properties for various load configurations.

that cracked hybrid fiber reinforced concrete is an aniso-tropic material and its response depends on the orientation of the predamage.[25]

Influence of coexisting biaxial tension on shear response

H1.0STM and H1.0STC were tested under combined shear and biaxial tension in a ratio of 1:0.5. Their response was compared against their counterparts tested under pure shear, as shown in Fig. 11. The presence of tension resulted in increased principal tensile stress at lower shear stresses. Hence, the panels cracked earlier and they failed as soon as the concrete toughness in tension was exhausted. The shear strength reduction was about 35%. The corresponding reduc-

tion in the ultimate deformation was 60%. As expected, the crack widths and crack spacings were larger for the panels subjected to co-acting biaxial tension when compared to pure shear panels H1.0PSM and H1.0PSC at the same shear stress levels.

CONCLUSIONS

Fourteen panel elements reinforced with conventional steel bars and steel fibers were tested in this study under well-defined shear loading conditions. Five variables were examined: total fiber volumetric fraction V_f; performance of the HySFRC specimens versus their monofiber counterparts with the same total amount of fibers; performance of panels tested under monotonic pure shear versus reversed cyclic
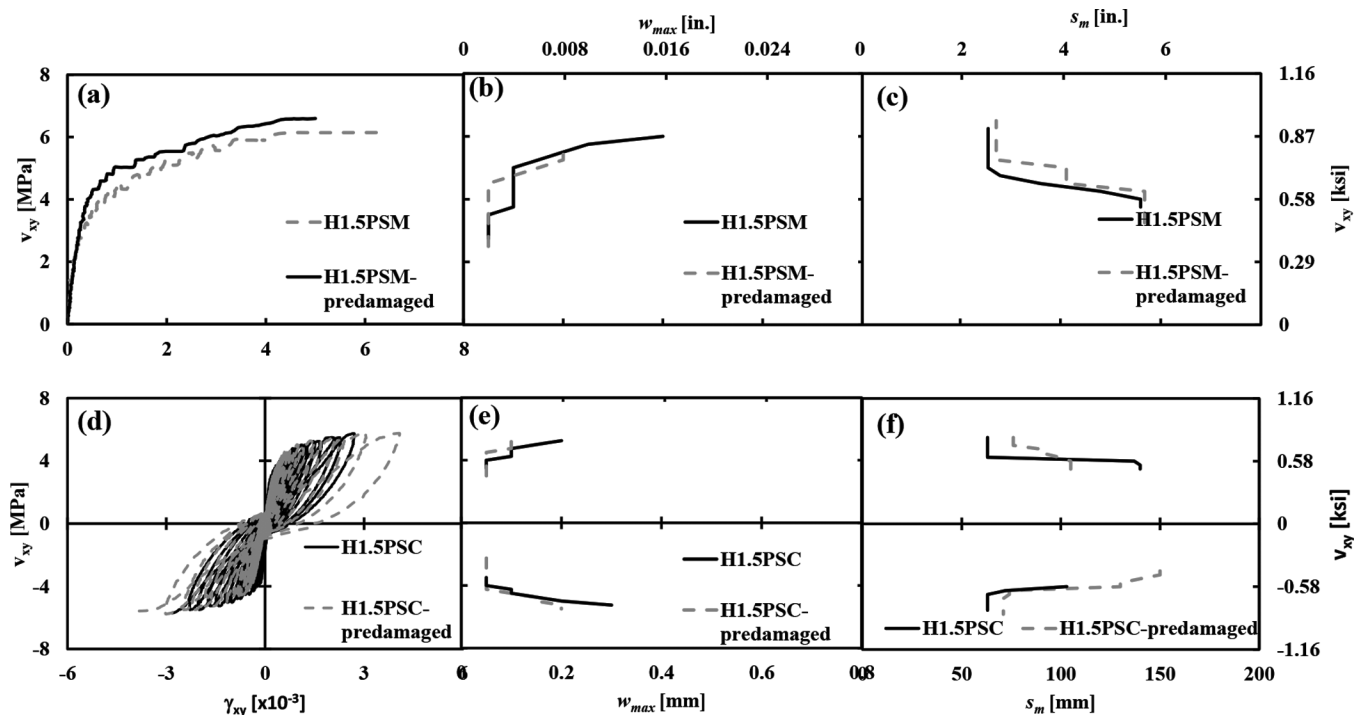
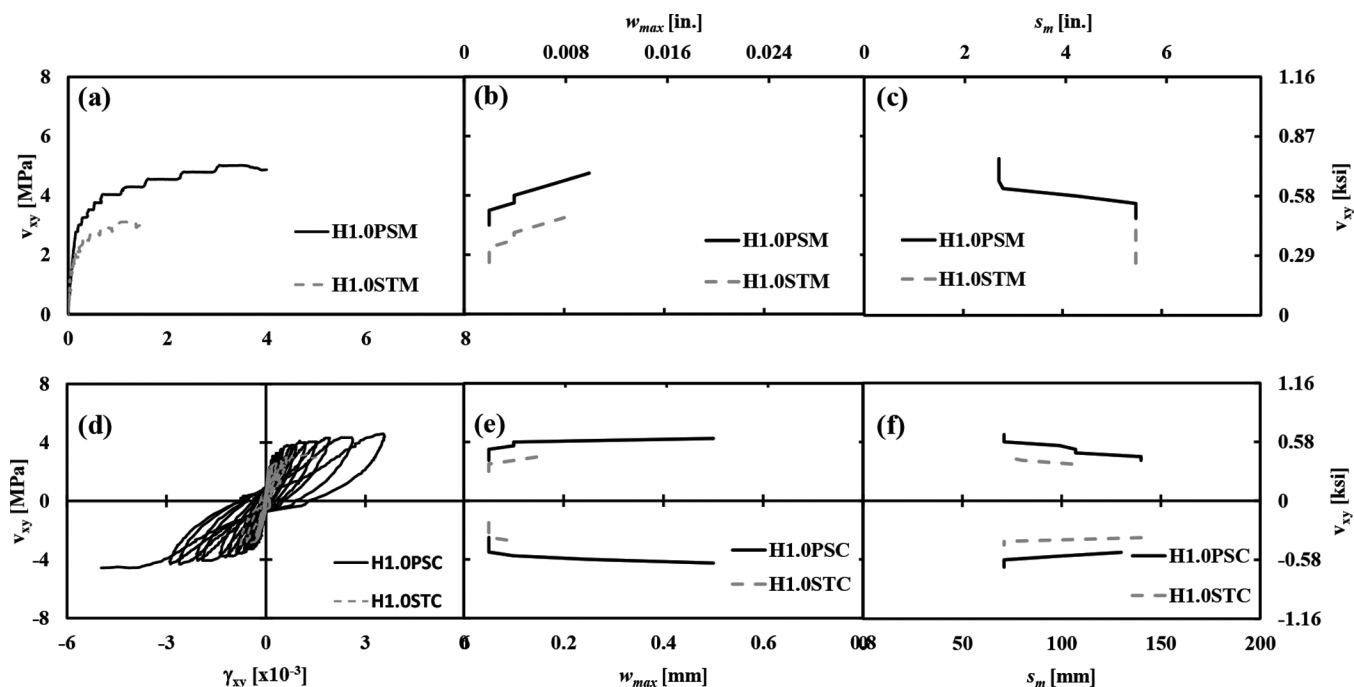Fig. 10—Influence of pre-cracking on panel shear response and cracking properties.

Fig. 11—Influence of simultaneous biaxial tension on panel shear response and cracking properties.

shear loading; panels that were cracked in longitudinal tension prior to shear loading versus initially uncracked panels; and the influence of proportionally increasing biaxial tension and shear on the panel response. From the results of the experimental investigation, the following conclusions are drawn:

1. Increasing the total fiber volumetric fraction in HySFRC leads to enhancements in shear strength, deformation capacity and stiffness. Greater concrete toughness due to higher amounts of fibers result in lower axial straining of the conventional reinforcement and therefore crack spacing and crack widths are also decreased. Crack stabilization is delayed with increasing V_f.

2. Fiber hybridization benefited performance both at the serviceability limit state (SLS), increasing the post-cracking stiffness, and at the ultimate limit state (ULS), increasing shear strength and deformation capacity relative to the monofiber counterparts. The synergy effect in shear increased with increasing fiber ratio. Crack widths and crack

spacings were also reduced with fiber hybridization. Stabilization was not affected.

3. The lower levels of shear deformation derived from fiber hybridization also resulted in smaller residual deformations upon unloading. Limited drift and improved damage control—key challenges in the design of reinforced concrete structures—can thus be more achievable by employing HySFRC.

4. Strength and deformation degradation due to cyclic damage accumulation appeared to take place during the last load steps before failure compared to the monotonic tests. Nevertheless, reductions in strength were limited to 6.5% and 4% for the HySFRC panels with 1.5% and 1.0% fibers, respectively. Cracking properties were not affected by load reversals.

5. Pre-cracking in tension affected the behavior under monotonic shear loading; strength and stiffness enhancement was observed although deformation capacity was reduced. An opposite effect was observed in the case of reversed cyclic shear. In both cases, larger crack spacings and smaller crack widths were observed over the course of the experiment. Tests results indicate that cracked hybrid fiber reinforced concrete is an anisotropic material and its response depends on the orientation of the predamage.

6. Co-acting biaxial tension caused a rise in the principal tensile stress at lower shear stress demand. As a result, cracking occurred earlier, and shear strengths and shear deformation capacities were reduced.

AUTHOR BIOS

*ACI member **Stamatina G. Chasioti** is a PhD Candidate at the University of Toronto, Toronto, ON, Canada. She received her bachelor's and master's degrees from Democritus University of Thrace, Xanthi, Greece. Her research interests include analysis and modeling of concrete structures using novel materials, reinforced concrete mechanics, and constitutive modeling.*

Frank J. Vecchio, *FACI, is a Professor in the Department of Civil Engineering at the University of Toronto. He is a member of Joint ACI-ASCE Committees 441, Reinforced Concrete Columns, and 447, Finite Element Analysis of Reinforced Concrete Structures. His research interests include nonlinear analysis and design of reinforced concrete structures, constitutive modeling, performance assessment and forensic investigation, and repair and rehabilitation of structures.*

ACKNOWLEDGMENTS

NOTATION

AR_f = fiber aspect ratio
A_s = reinforcing bar cross-sectional area
d_b = reinforcing bar diameter
d_f = fiber diameter
E_f = fiber modulus of elasticity
E_s = reinforcing bar steel modulus of elasticity
$f_{ck,100}$ = compressive strength of concrete obtained from cylinders
f_u = reinforcing bar fracture strength
f_{uf} = fiber ultimate tensile strength
f_y = reinforcing bar yield strength
l_f = fiber length
s_m = mean crack spacing at failure
V_f = total fiber volumetric ratio (w/w)
v_{cr} = shear stress at onset of cracking
v_u^+ = ultimate shear stress in positive shear
v_u^- = ultimate shear stress in negative shear
w_{max} = maximum crack width recorded
ε_y = reinforcing bar yield strain
ε_u = reinforcing bar fracture strain
γ_{cr} = shear strain at onset of cracking
γ_u^+ = ultimate shear strain in positive shear
γ_u^- = ultimate shear strain in negative shear
ρ_x = reinforcement ratio in x-direction
ρ_y = reinforcement ratio in y-direction

REFERENCES

1. Balaguru, P. N., and Shah, S. P., *Fiber Reinforced Cement Composites*, McGraw Hill, New York, 1992, 531 pp.

2. Bentur, A., and Mindess, S., *Fiber Reinforced Cementitious Composites*, Elsevier Applied Science, London, UK, 1990, 624 pp.

3. Taya, M., and Arsenault, R. J., *Metal Matrix Composites*, first edition, Pergamon Press, Oxford, UK, 1989, 274 pp.

4. Banthia, N., and Sappakittipakorn, M., "Toughness Enhancement in Steel Fiber Reinforced Concrete Through Fiber Hybridisation," *Cement and Concrete Research*, V. 37, No. 9, 2007, pp. 1366-1372. doi: 10.1016/j.cemconres.2007.05.005

5. Xu, G.; Magnani, S.; and Hannant, D. J., "Durability of Hybrid Polypropylene-Glass Fiber Cement Corrugated Sheets," *Cement and Concrete Composites*, V. 20, No. 1, 1998, pp. 79-84. doi: 10.1016/S0958-9465(97)00075-9

6. Shah, S. P., "Do Fibers Increase the Tensile Strength of Cement-Based Matrix?" *ACI Materials Journal*, V. 88, No. 6, Nov.-Dec. 1991, pp. 595-602.

7. Chasioti, S. G., and Vecchio, F. J., "Hybrid Steel Fiber Reinforced Concrete panels in Shear: Experimental Investigation," *Proceedings of the 7th RILEM Conference on High-Performance Fiber-Reinforced Cement Composites*, Stuttgart, Germany, 2015, pp. 351-358.

8. Lawler, J. S.; Zampini, D.; and Shah, S. P., "Microfiber and Macrofiber Hybrid Fiber-Reinforced Concrete," *Journal of Materials in Civil Engineering*, ASCE, V. 17, No. 5, 2005, pp. 595-604. doi: 10.1061/(ASCE)0899-1561(2005)17:5(595)

9. Naaman, A. E., and Reinhardt, H. W., "Setting the Stage: Toward Performance Based Classification of FRC Composites," *Proceedings of the 4th RILEM Conference on High-Performance Fiber-Reinforced Cement Composites*, Ann Arbor, MI, 2003, pp. 1-4.

10. Naaman, A. E., and Reinhardt, H. W., "Proposed Classification of HPFRC Composites Based on Their Tensile Response," *Materials and Structures*, V. 39, No. 5, 2006, pp. 547-555. doi: 10.1617/s11527-006-9103-2

11. Blunt, J., and Ostertag, C. P., "Performance-Based Approach for the Design of a Deflection Hardened Hybrid Fiber-Reinforced Concrete," *Journal of Engineering Mechanics*, ASCE, V. 135, No. 9, 2009, pp. 978-986. doi: 10.1061/(ASCE)0733-9399(2009)135:9(978)

12. Aoude, H.; Belghiti, M.; Cook, W. D.; and Mitchell, D., "Response of Steel Fiber-Reinforced Concrete Beams with and without Stirrups," *ACI Structural Journal*, V. 109, No. 3, May-June 2012, pp. 359-367.

13. Minelli, F., and Plizzari, G. A., "On the Effectiveness of Steel Fibers as Shear Reinforcement," *ACI Structural Journal*, V. 110, No. 3, May-June 2013, pp. 379-389.

14. Meda, A.; Minelli, F.; Plizzari, G. A.; and Riva, P., "Shear Behaviour of Steel Fibre Reinforced Concrete Beams," *Materials and Structures*, V. 38, No. 3, 2005, pp. 343-351. doi: 10.1007/BF02479300

15. Parra-Montesinos, G. J., "Shear Strength of Beams with Deformed Steel Fibers," *Concrete International*, V. 28, No. 11, Nov. 2006, pp. 57-66.

16. ACI Committee 318, "Building Code Requirements for Structural Concrete and Commentary (ACI 318-08)," American Concrete Institute, Farmington Hills, MI, 2005, 465 pp.

17. ASTM C1609/C1609M, "Standard Test Methods for Flexural Performance of Fiber-Reinforced Concrete (Using Beam with Third-Point Loading)," ASTM International, West Conshohocken, PA, 2013, 9 pp.

18. RILEM TC 162-TDF., "RILEM TC 162-TDF: Test and Design Methods for Steel Fibre Reinforced Concrete," *Materials and Structures*, V. 36, No. 262, 2003, pp. 560-567. doi: 10.1617/14007

19. Li, V. C.; Mishra, D. K.; Naaman, A. E.; Wight, J. K.; LaVave, J. M.; Wu, H.-C.; and Inada, Y., "On the Shear Behavior of Engineering Cementitious Composites," *Journal of Advanced Cement Based Materials*, V. 1, No. 3, 1994, pp. 142-149. doi: 10.1016/1065-7355(94)90045-0

20. Panagiotou, M.; Trono, W.; Jen, G.; Kumar, P.; and Ostertag, C. P., "Experimental Seismic Response of Hybrid Fiber-Reinforced Concrete Bridge Columns with Novel Longitudinal Reinforcement Detailing," *Journal of Bridge Engineering*, ASCE, V. 20, No. 7, 2014, doi: 10.1061/(ASCE)BE.1943-5592.0000684

21. Buzzini, D.; Dazio, A.; and Trüb, M., *Quasi-Static Cyclic Tests on Three Hybrid Fibre Concrete Structural Walls*, Intitiut für Baustatik und Konstruktion Bericht, ETH Zürich, Zürich, Switzerland, 2006. doi:10.3929/ethz-a-005195397.10.3929/ethz-a-005195397

22. CSA A23.1-09/A23.2-09, "Concrete Materials and Methods of Concrete Construction/Test Methods and Standard Practices for Concrete," Canadian Standards Association, Toronto, ON, Canada, 2009, 674 pp.

23. ASTM C469/C469M, "Standard Test Method for Static Modulus of Elasticity and Poisson's Ratio of Concrete in Compression," ASTM International, West Conshohocken, PA, 2014, 5 pp.

24. Pimanmas, A., and Maekawa, K., "Influence of Pre-Cracking on Reinforced Concrete Behavior in Shear," *Proceedings of JSCE*, No. 38, 2001, pp. 207-223.

25. Suryanto, B.; Nagai, K.; and Maekawa, K., "Bidirectional Multiple Cracking Tests on High-Performance Fiber-Reinforced Cementitious Composite Plates," *ACI Materials Journal*, V. 107, No. 5, Sept.-Oct. 2010, pp. 450-460.